

The nature and fate of natural resins in the geosphere. Part X.[‡] Structural characteristics of the macromolecular constituents of modern Dammar resin and Class II ambers

Ken B. Anderson* and John V. Muntean

Chemistry Division, Argonne National Laboratory, Argonne, IL, 60439, USA

E-mail: kbanderson@anl.gov

Article

Received 11th January 2000, Accepted 25th January 2000

Published on the Web 2nd March 2000

As part of a larger study of the structure and behavior of polyterpenoids in sedimentary systems, the structural characteristics of the macromolecular constituents of Dammar resin and a related Class II amber have been reinvestigated. The conclusions drawn from these analyses are inconsistent with the current widely held "polycadinene" model for the macromolecular structure of these materials. Double bond characteristics observed by one and two dimensional NMR spectroscopy do not match those in the proposed "polycadinene" structure. Based on these observations it is suggested that the proposed "polycadinene" structure for these materials is inadequate and requires revision. Elemental and NMR data also suggest a significant contribution from functionalized monomers.

Introduction

Class II ambers, although apparently less abundant than class I ambers on a global scale, are nonetheless important constituents of sedimentary organic matter in several regions; SE Asia and Central and SE North America in particular. These materials have been widely reported to be the major source material for the bicadinanes (Fig. 1, I and II) which are found in many crude oils and which are widely used as markers of maturity and terrestrial input.²⁻¹⁰

Ambers of this class have been shown to be composed of both a low MW fraction and a high MW macromolecular phase.¹¹⁻¹⁵ Extensive analyses of the low MW fraction have identified a large number of functionalized sesqui- and triterpenoids, primarily of the cadinane, oleanane and dammarane skeletal types.^{12,16-18} It is believed that the bicadinanes observed in source rock extracts and crude oils are derived from the HMW fraction of the amber. The current prevailing view of the nature of the HMW fraction, proposed by van Aarssen and coworkers,^{3,12-15} is that this is composed predominantly of a cadinene polymer, loosely referred to as "polycadinene" (Fig. 1, III). Although it is difficult to rationalize the formation of III under natural conditions from biologically reasonable precursors without invoking enzymatic processes¹² the structure proposed by these authors preserves the "methylene bridged" character observed in the bicadinanes, and readily rationalizes the observed formation of bicadinanes on thermolysis of the macromolecular phase.

It has been shown that the distribution of bicadinane isomers in source rock extracts varies as a direct function of maturity,⁸ which is consistent with the view that these products, and related unassigned "dimers" and higher homologues, are derived by thermal disruption of the HMW component of these ambers. This view also implies that the structural characteristics of these products are directly related to the structure of the HMW material.^{2,3} However, in order to establish this, it is necessary to have detailed knowledge of the structural characteristics of this HMW material.

In the present study, the structural characteristics of the macromolecular constituents of modern and fossil Dammar have

been reinvestigated using high resolution one and two dimensional (1 and 2D) NMR techniques. Effort has focused primarily on investigation of the characteristics of olefinic structures, with the intent of refining details of the overall structural characteristics of these polymers.

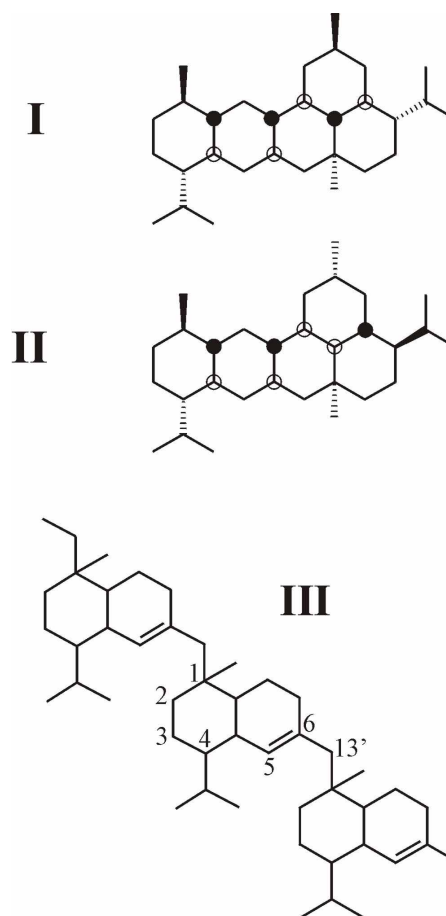


Fig. 1 Structures of *trans-trans,trans*-bicadinane (I), *cis-cis-trans*-bicadinane (II) and polycadinene (as proposed by van Aarssen *et al.*¹²) (III).

[‡] For Part IX see ref. 1

Experimental

Modern "undewaxed" commercial Dammar was purchased from Sigma Chemical Co. Miocene Dammar from the Merit Pila Coal mine was obtained from a commercial amber dealer.

Dammar resin (10 g) was dissolved in CH_2Cl_2 (50 mL) with sonication. This solution was then filtered to remove extraneous materials, and the filtrate concentrated to a small volume by rotary evaporation. To this concentrate, CH_3OH (100 mL) was then added in small portions to give a white precipitate, which was then recovered by filtration. The precipitate was then resuspended in CH_3OH and sonicated to ensure complete removal of CH_3OH soluble materials. The product was recovered by filtration and dried. Yield = 9.5 g.

Attempts to recover fossil Dammar polymer by the procedure used for the modern Dammar were unsuccessful due to the presence of substantial amounts of CH_2Cl_2 insoluble materials which made filtration impossible. Therefore, amber (9.9 g) was placed in a Gregar extractor and extracted with CH_2Cl_2 (150 mL) for 24 h. The extract was then worked up as described above. Yield = 6.4 g.

Products from both the modern and fossil Dammar were subjected to analytical pyrolysis at 300 °C, in the presence of tetramethyl ammonium hydroxide (TMAH),¹⁹ to check for the presence of volatile impurities. No products of significant abundance were observed.

All NMR experiments were performed on a Bruker model DMX 500 NMR spectrometer (11.7 T). With the use of the nitrogen pre-cooler, heater coil, and the variable temperature controller, the temperature was stable at 294.3±0.1 K. The ^{13}C NMR spectra and the DEPT (distortionless enhancement by polarization transfer)²⁰ spectra were recorded with a two channel 10 mm broadband, direct detection, variable temperature probe with proton decoupling and ^1H lock at 76.773 MHz. Inverse gated proton decoupling was accomplished *via* the WALTZ 16 sequence.²¹⁻²³ ^{13}C spectra were recorded with 22,000 acquisitions, 10 s recycle delay, 9 μs pulse width (70°) and 33 kHz sweep width. DEPT spectra were recorded with 12,000 acquisitions, 10 s recycle delay, and 42 kHz sweep width.

For the ^1H , COSY, HMQC, and HMBC experiments, (see below) a three channel 5 mm inverse detection, three axis gradient, variable temperature probe with ^2H lock at 76.773 MHz was used. ^1H spectra were recorded with 1000 acquisitions, 4 s recycle delay, 4 μs pulse width (70°) and 6 kHz sweep width. COSY (correlated spectroscopy)^{24,25} spectra were recorded with gradient phase cycling, 200 acquisitions and 1 K data over 3.2 kHz in the F_2 dimension, and 4 s recycle delay. The F_1 dimension covered 3.2 kHz sweep width with 256 increments. Fourier transformed data were zero filled to 1 K by 1 K points. The ^1H 90° pulse was 6.75 μs .

HMQC (heteronuclear multiple quantum correlation)^{26,27} and HMBC (heteronuclear multiple bond correlation)^{27,28} spectra were recorded with gradient phase cycling, 260 acquisitions and 2 K data over 3.8 kHz in the F_2 (^1H) dimension, and 1.5 s recycle delay. The F_1 (^{13}C) dimension covered 33 kHz sweep width with 128 increments. Fourier transformed data were zero filled to 2 K by 1 K points. The ^{13}C and ^1H 90° pulses were 12.25 and 6.75 μs respectively. Proton decoupling was accomplished *via* the GARP composite sequence²⁹ and a coupling constant of 145 Hz was used in the HMQC experiment. A delay corresponding to a 20 Hz coupling was used to select long range couplings in the HMBC experiment.

Results and discussion

Conventional ^1H and ^{13}C spectra for both modern and fossil Dammar are illustrated in Fig. 2 and 3 respectively. ^{13}C spectra were collected in both CDCl_3 (Fig. 3i and ii) and CD_2Cl_2 (Fig. 3iii) to ensure observation of all carbons. DEPT 45, 90 and

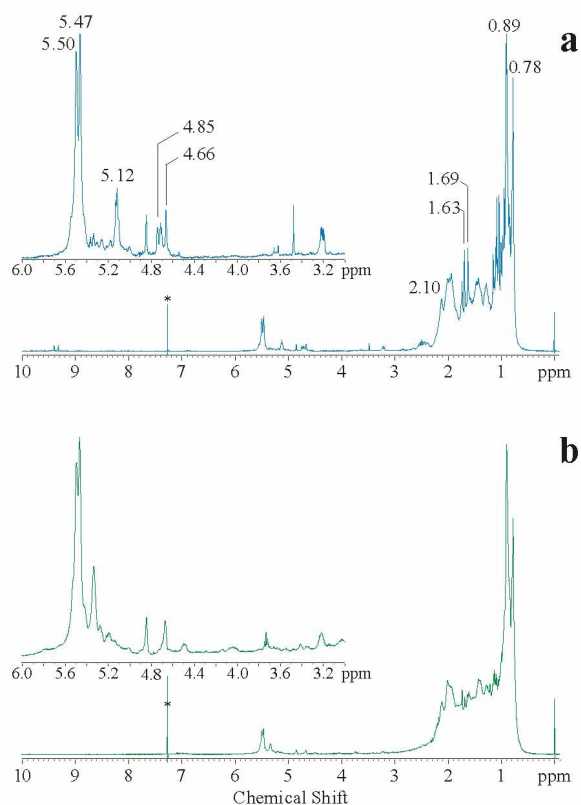


Fig. 2 1D ^1H NMR spectra for modern (a) and fossil (b) Dammar polymers. Details of olefinic proton resonances are inset for clarity (*= CHCl_3). Click to access interactive NMR spectra for (a) and (b).

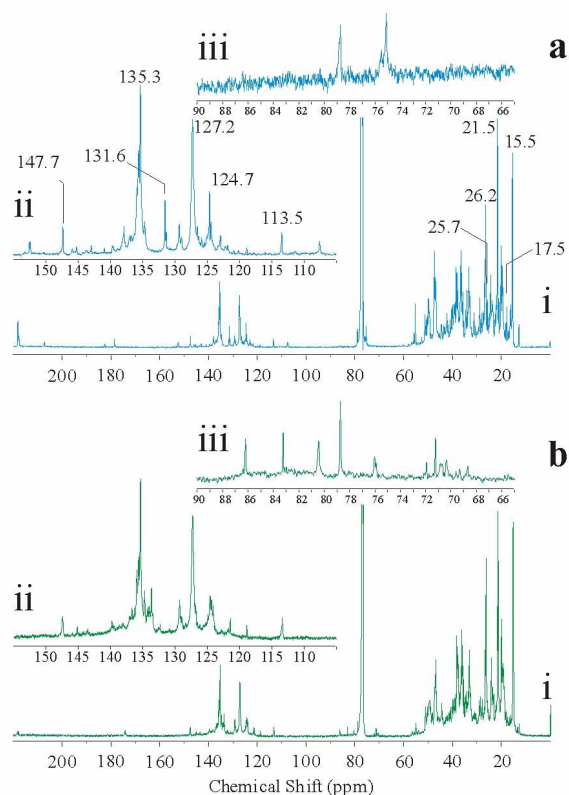


Fig. 3 1D ^{13}C NMR spectra for modern (a) and fossil (b) Dammar polymers. Enlargements showing details of olefinic resonances (ii) are inset, as are details of the 95-65 ppm region showing details of alcohol/ether resonances, measured in CD_2Cl_2 (iii). Click to access interactive NMR spectra for 3ai and 3aii, 3aiii, 3bi and 3bii and 3biii.

^{13}C analyses (Fig. 4 and 5) were also carried out to provide confirmatory data for the assignment of carbon types as quaternary, methine, methylene, or methyl.

The data illustrated in Fig. 2 and 3 are similar to data previously reported for comparable samples.¹² Integration data for the modern Dammar polymer show $\text{H}_{\text{olefin}}:\text{H}_{\text{total other}}=1:27.1$, slightly less than the value (*ca.* 1:23) reported by van Aarssen and coworkers.¹² The $\text{C}_{\text{olefin}}:\text{C}_{\text{total other}}$ ratio (1:9.5) is also slightly less than the 1:7.5 required by the prevailing polycadinene model (III).

It is also apparent from the data illustrated in Fig. 2 and 3 that a significant number of oxygen containing functional groups are present in both the modern and fossil polymers. Resonances due to alcohols ($^{13}\text{C}=90\text{-}65$ ppm), carboxy ($^{13}\text{C}=185\text{-}170$ ppm), aldehydes ($^{13}\text{C}=207$ ppm) and ketones ($^{13}\text{C}=220$ ppm) are all readily apparent in these data. Although individually minor, in sum, these resonances represent a significant structural element. This contention is supported by elemental analyses (Table 1) which suggests the presence of ~5.5 wt.% O.

1D NMR spectra provide excellent information regarding the distribution of carbon and proton types within a sample, but they do not directly provide evidence of either C-C or C-H connectivity. In simple molecules, connectivity can usually be inferred from chemical shift arguments and in many cases structures can be unambiguously assigned from these data alone. In the case of more complex systems, such as those with which the present study is concerned, chemical shift arguments are less definitive. In such cases it is necessary to use 2D analyses in order to derive unambiguous structural assignments.

2D NMR analyses depend on transfer of magnetization from one nuclei to adjacent or more remote nuclei. Those used in this study all rely on transfer of magnetization through covalent bonds and hence provide direct evidence of connectivity. There are a number of different types of 2D NMR experiments which provide complimentary evidence of C-H and H-C_n-H connectivity. HMQC analyses are used to observe correlations between ^{13}C and ^1H through a single covalent bond, usually abbreviated as $^1J_{\text{C-H}}$. HMBC analyses also provide information concerning C-H connectivity, but in this case NMR parameters are set such that two and three bond ($^2J_{\text{C-H}}$ and $^3J_{\text{C-H}}$) correlations are detected. That is, correlations are observed between ^1H nuclei and ^{13}C adjacent to (and twice removed from), the carbon to which the proton is directly covalently bound. COSY data detect $^2J_{\text{H-H}}$ and $^3J_{\text{H-H}}$ correlations and hence show correlations between geminal protons (protons attached to the same carbon) and protons attached to adjacent carbons (note: in order to be observable, geminal protons must be magnetically inequivalent). When taken together, these data sets provide compelling and complementary evidence for C-C and C-H 1, 2 and 3 bond connectivity.

In principle, it should be possible to use these data sets to establish the connectivity (and hence the structural environment) of all atoms in the structure using a build-on-the-chain approach. To illustrate by example: strong resonances are observed in the ^1H spectra of the modern polymer (Fig. 2) at 0.78 and 0.89 ppm. Using 2D analyses (see Fig. 6) it is possible to determine the precise characteristics of the protons giving rise to these intense resonances. From HMQC data (Fig. 6a), these resonances correspond to ^{13}C resonances at 15.5 and 21.5 ppm respectively. From chemical shift considerations (and confirmed from DEPT data, Fig. 4), it is clear that both of these resonances ($^{13}\text{C}=15.5$, $^1\text{H}=0.78$ ppm and $^{13}\text{C}=21.5$, $^1\text{H}=0.89$ ppm) are attributable to CH_3 groups. HMBC data for this sample (Fig. 6b) indicate that the ^1H resonance at 0.78 ppm correlates ($^2J_{\text{C-H}}$ and $^3J_{\text{C-H}}$) with ^{13}C resonances at 21.5 and 26.2 ppm, while the ^1H resonance at 0.89 ppm correlates ($^2J_{\text{C-H}}$ and $^3J_{\text{C-H}}$) with ^{13}C resonances at 15.5 and 26.2 ppm. HMQC data (Fig. 6a) establish that the ^{13}C resonance at 26.2 ppm is

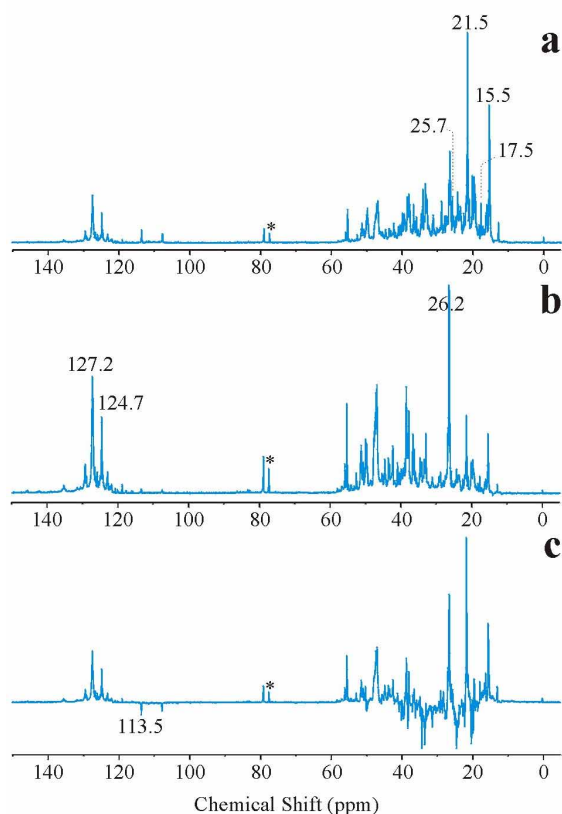


Fig. 4 DEPT spectra for modern Dammar polymer. (a) DEPT 45 (all protonated carbon), (b) DEPT 90 (CH, methyl resonances may also still be observed but are greatly attenuated), (c) DEPT 135 (CH and CH_2 resonances appear as negative) ($^*\text{=CHCl}_3$). Click to access interactive NMR spectra for (a), (b) and (c).

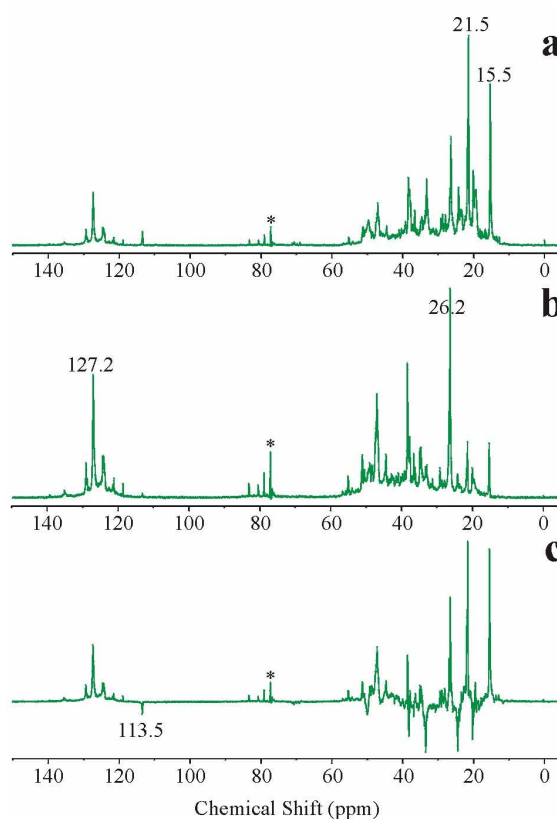


Fig. 5 DEPT spectra for modern fossil Dammar polymer. (a) DEPT 45, (b) DEPT 90, (c) DEPT 135 (See also caption for Fig. 4 for additional description) ($^*\text{=CHCl}_3$). Click to access interactive NMR spectra for (a), (b) and (c).

Table 1 Elemental analyses^a

Sample	C (wt.%)	H (wt.%)	N (wt.%)	O+S (wt.%) ^b	Nominal formula (based on C ₁₅)
Modern Dammar polymer	83.7	10.7	<0.05	5.6	C ₁₅ H ₂₃ (O + S) _{0.75}
Fossil Dammar polymer	84.2	10.4	<0.05	5.4	C ₁₅ H ₂₂ (O + S) _{0.72}
Polycadinene (III) ^c					C ₁₅ H ₂₄

^aAll data are averages of at least 4 analyses. ^bBy difference. ^cRef. 12.

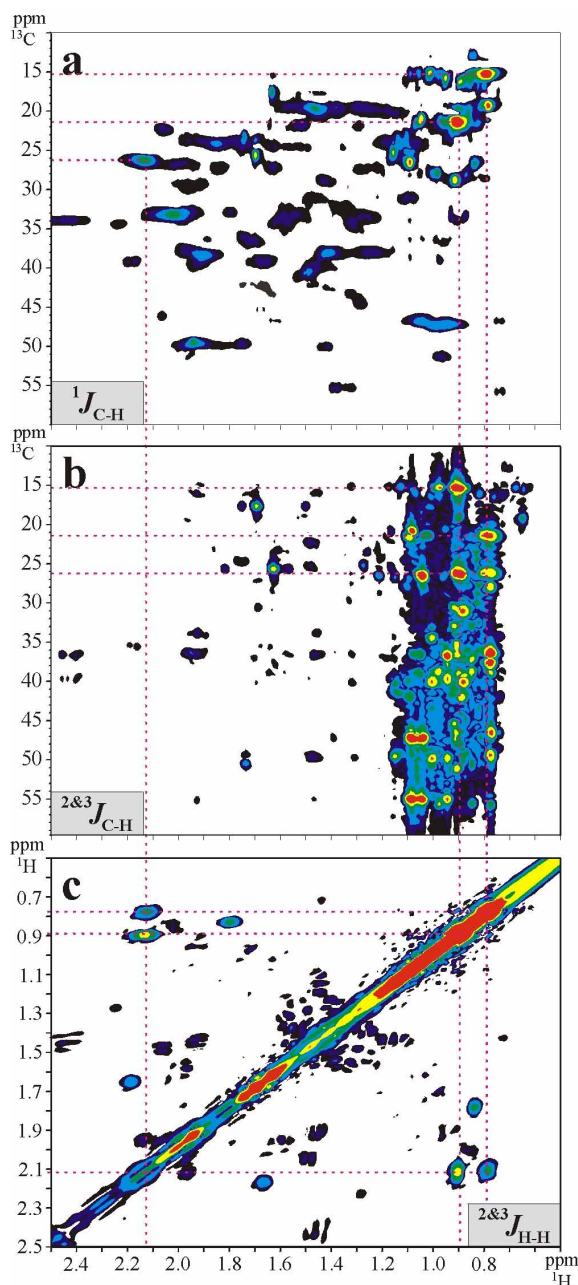


Fig. 6 2D ¹³C-¹H NMR spectra for modern Dammar polymer. (a) HMQC, (b) HMBC and (c) COSY. Correlating resonances due to an isopropyl structure are indicated by dashed lines. Click on the image or [here](#) for a larger view.

coupled (¹J_{C-H}) to a ¹H resonance at 2.10 ppm. DEPT data (see Fig. 4) and chemical shift both indicate that these signals (¹³C=26.2, ¹H=2.10) arise from a CH structure. COSY data (Fig. 6c) show that the ¹H resonance at 2.10 ppm correlates (³J_{H-H}) with both of the ¹H resonances at 0.78 and 0.89 ppm,

which confirms that the ¹³C=26.2 ppm methine structure is α to both of the methyl groups, ¹³C=15.5, ¹H=0.78 ppm and ¹³C=21.5, ¹H=0.89 ppm. Hence, taken in sum, these data indicate that the two methyl groups (¹³C=15.5 and 21.5 ppm) are attached to the methine carbon (¹³C=26.2 ppm). That is, these three pairs of resonances and their correlations and cross-correlations unambiguously derive from the presence of an isopropyl group, as illustrated in Fig. 7. (The magnetic inequivalence of the methyl groups is almost certainly due to hindered rotation of the isopropyl structure, as has been observed in related terpene systems.²⁰)

Although the process can be somewhat complex, by examining correlations and cross-correlations in this manner, contiguous chain information may be built up, and structural elements can often be identified with confidence, even in complex systems. Unfortunately, in the polymer systems characterized in this study it is not possible to completely establish all connectivities due to coincidental overlap of resonances arising from chemically similar but discontinuous structures. Nevertheless it is possible to unambiguously establish the nature of a number of key structural elements, most notably olefinic structures and several of the oxygenated structures. The remainder of this report will focus on analysis of olefinic structural elements.

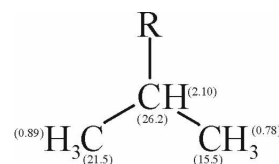


Fig. 7 Isopropyl structure, with ¹³C and ¹H resonances observed in Dammar polymer indicated. Move your mouse over the atom to see the NMR resonances.

Olefinic structures

¹H and ¹³C spectra (Fig. 2 and 3 respectively) clearly indicate the presence of a number of olefinic structures in both the modern and fossil polymers (¹H = 6.0-3.1 ppm, ¹³C = 155-105 ppm). The ¹³C spectra for the modern Dammar polymer shows 2 predominant olefin resonances at 127.2 and 135.3 ppm (with some indication of multiple overlapping resonances), and with secondary olefinic resonances at 124.7 and 131.6 ppm. Additional minor olefinic resonances are also observed. Chemical shift considerations and DEPT data (Fig. 4) indicate that the resonances at 135.3 and 131.6 ppm are due to nonprotonated olefinic carbons and the 127.2 and 124.7 ppm resonances arise from protonated olefinic carbons.

Consider first the structure of the most abundant (primary) olefin. The deduced structural environment of this olefin is illustrated in Fig. 8. The basis for this assignment is as follows: taking as a starting point the protonated olefinic ¹³C resonance at 127.2 ppm, HMQC data (Fig. 9a) indicate that this resonance corresponds to both of the ¹H resonances at 5.47 and 5.50 ppm. (This multiplicity has been observed previously and has been

shown not to result from spin coupling.¹²) It is very likely that the apparent "splitting" of this proton resonance is the result of differences in the stereochemical configuration of the α aliphatic carbon. HMBC data (Fig. 9b) indicate a complete absence of $^2J_{C-H}$ and $^3J_{C-H}$ couplings to the ^{13}C 127.2 ppm resonance and COSY data (Fig. 9d) show no $^3J_{H-H}$ correlations between the 1H resonances at 5.47 and 5.50 ppm and other 1H signals. (The minor correlation at ~ 2.2 and 5.5 ppm is due to coupling between the ~ 5.5 ppm proton associated with the ^{13}C resonating at ~ 129 ppm and the 1H of an unidentified aliphatic structure.)

The absence of correlations between the 1H and ^{13}C of the protonated olefinic carbon of this structure and α 1H indicates that there are no protons on the carbon α to the protonated olefinic carbon. That is, the aliphatic carbon alpha to the protonated olefinic carbon is quaternary. This assignment is further supported by the observation of $^2J_{C-H}$ and $^3J_{C-H}$ couplings between the olefinic proton ($^1H = 5.47$ and 5.50 ppm) and four aliphatic ^{13}C resonances (Fig. 9c, 33.2, 38.5,

46.9 and 49.7 ppm). The existence of four such couplings confirms the quaternary nature of the carbon α to $^{13}C = 127.2$ ppm. Hence the structural nature of the most abundant (primary) olefin must be as indicated in Fig. 8.

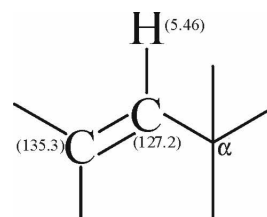


Fig. 8 Structural characteristics of the primary olefin present in modern and fossil Dammar polymers. Move your mouse over the atom to see the NMR resonances.

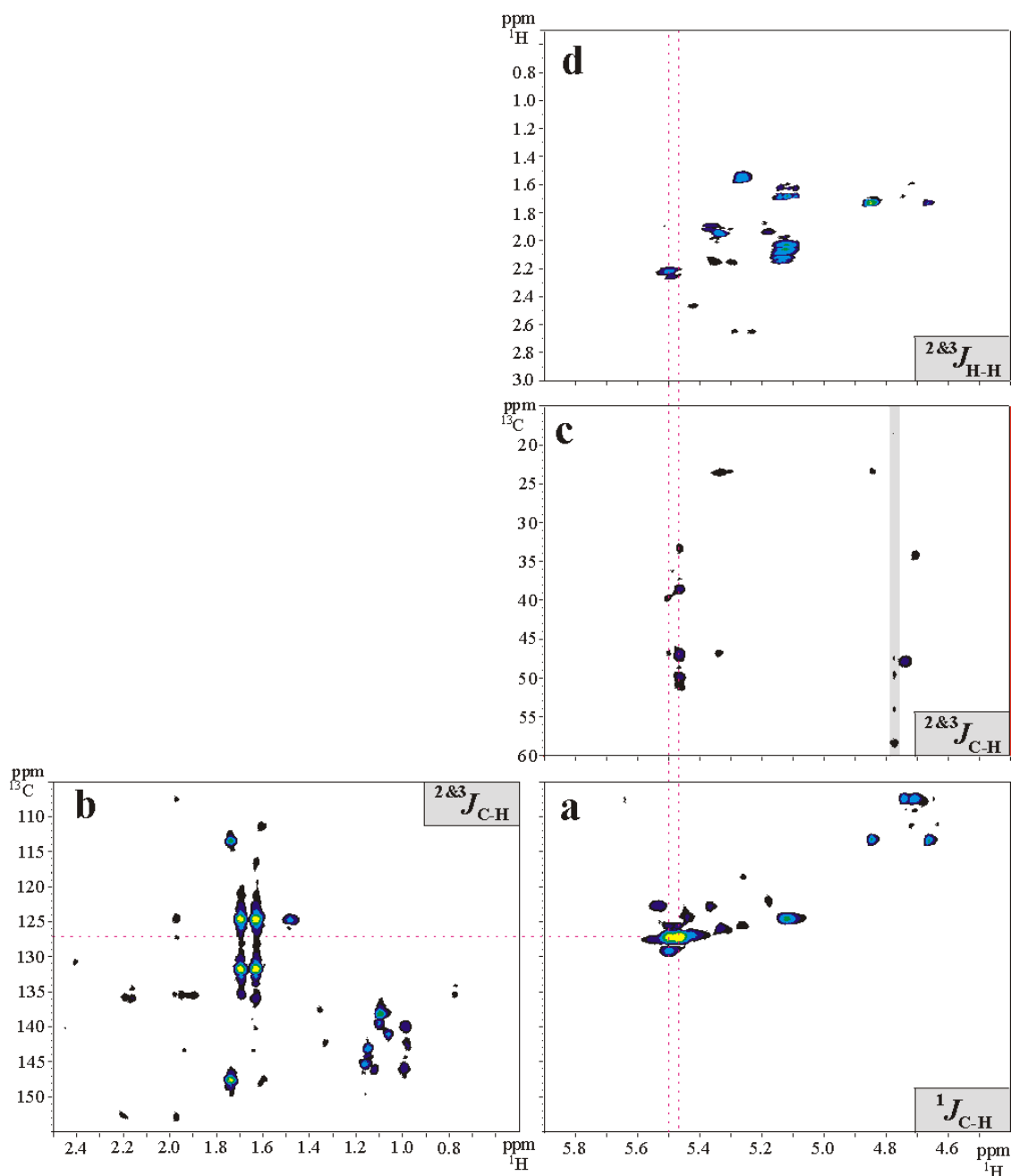


Fig. 9 2D ^{13}C - 1H NMR spectra for modern Dammar polymer. (a) HMQC, (b) and (c) HMBC and (d) COSY. Resonances due to the primary olefinic structure are indicated by dashed lines. Click on the image or [here](#) for a larger view.

As noted above, analyses such as those used in the present study depend on the transfer of magnetization from one nuclei to adjacent or more remote nuclei. The magnitude of any given coupling is determined by the coupling constants between the nuclei, and by loss of magnetization due to relaxation. Therefore, to ensure that the absence of detectable couplings to the ^{13}C 127.2 ppm resonance does not result from rapid relaxation of the ^1H magnetization, ^1H T_1 measurements were taken for the olefinic protons of both the primary and secondary olefinic structures. The results of these measurements are as follows: $^1\text{H}_{\text{Primary olefinic}}=670$ ms, $^1\text{H}_{\text{Secondary olefinic}}=1100$ ms. Both of these measurements are well within the range detectable in these experiments. (The HMBC sequence used for these experiments requires only 107 ms before acquisition.) To even further ensure that correlations would be observable if they were present, ^1H T_1 experiments were also performed on a soluble polymer isolated from an immature Class I (polylabdanoid) resinite. ^1H T_1 values measured for the olefinic protons in this (polymeric) sample were found to be of the same order (800-1100 ms) as those of the olefinic ^1H of the present samples. COSY and HMBC correlations were readily observable in all cases, including $^2J_{\text{C-H}}$ to the protonated ^{13}C of the side-chain olefin from the adjacent methylene protons. It therefore appears that the absence of observable $^{2+3}J_{\text{C-H}}$ correlations to the protonated ^{13}C of the primary olefin in these samples is not an experimental artifact.

The structure proposed by van Aarssen and coworkers^{3,12-15} (Fig. 1, III) includes only one quaternary aliphatic carbon (carbon 1). In order to place the double bond illustrated in Fig. 8 into this skeleton it would be necessary to place it between carbon 6 and carbon 13'. This bond is integral to the backbone of the macromolecular structure. If the double bond were in this position then cleavage of the olefin by ozonolysis, or treatment

with other oxidants such as RuO_4 would lead to complete depolymerization of the structure. This is not observed.¹¹

The structural characteristics of the secondary olefin may be deduced in a similar manner. The protonated carbon of this structure resonates at 124.7 ppm. HMQC data (Fig. 10a) indicate that this carbon is coupled to the olefinic proton resonating at 5.12 ppm. Unlike the protonated carbon of the primary olefin, this carbon (124.7 ppm) shows strong $^2J_{\text{C-H}}$ and/or $^3J_{\text{C-H}}$ correlations with protons resonating at 1.63 and 1.69 ppm (Fig. 10b). These protons also correlate with the carbon resonance at 131.6 ppm which is clearly the non-protonated carbon of this olefinic structure.

HMQC data (Fig. 10c) indicate that these protons (1.63 and 1.69 ppm) are directly coupled to ^{13}C resonating at 17.5 and 25.7 ppm, respectively. It can be seen from the HMBC data for this sample (Fig. 10d) that these protons cross-couple. That is, (in addition to the olefinic carbons resonating at 124.5 and 131.6 ppm), the ^1H resonance at 1.63 ppm correlates $^3J_{\text{C-H}}$ only with the ^{13}C resonance at 25.7 ppm, and likewise, the protons resonating at 1.69 ppm correlate only with the ^{13}C resonance at 17.5 ppm. This cross-correlation confirms that the carbons giving rise to the resonances at $^{13}\text{C} = 17.5$ 25.7 ppm are connected through a single quaternary carbon (*viz.* $^{13}\text{C} = 131.6$ ppm).

The absence of additional $^2J_{\text{C-H}}$ and/or $^3J_{\text{C-H}}$ couplings from the protons associated with these carbons ($^1\text{H} = 1.63$ and 1.69 ppm) suggests that these structures are terminal. This conclusion is supported by DEPT data (Fig. 5) and chemical shift comparisons with comparable structures in other terpenes³⁰ which confirm that the $^{13}\text{C} = 17.5$, $^1\text{H} = 1.63$ ppm resonances and $^{13}\text{C} = 25.7$, $^1\text{H} = 1.69$ ppm resonances are due to methyl groups. Consequently, the structure of this olefin must be as illustrated in Fig. 11.

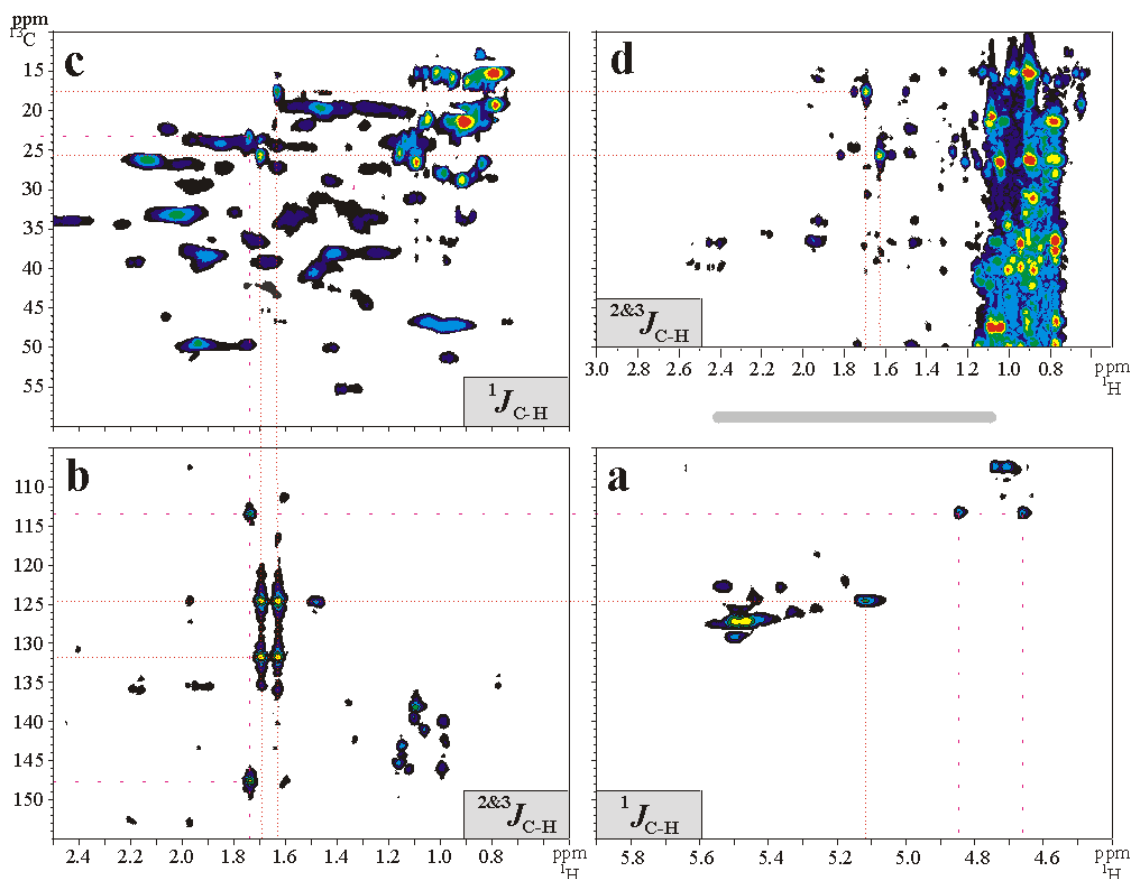


Fig. 10 2D ^{13}C - ^1H NMR spectra for modern Dammar polymer. (a) and (c) HMQC and (b) and (d) HMBC. Resonances due to the secondary olefinic structures are joined by dashed lines. Click on the image or [here](#) to access a larger view.

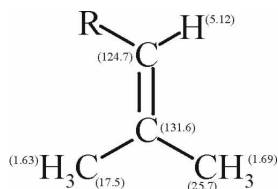


Fig. 11 Structural characteristics of the secondary olefin present in modern Dammar polymer. Move your mouse over the atom to see the NMR resonances.

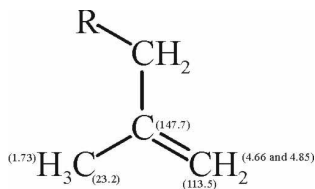


Fig. 12 Structural characteristics of a minor olefin present in modern Dammar polymer. This structure is isomeric with the secondary olefin illustrated in Fig. 11. Move your mouse over the atom to see the NMR resonances.

The data illustrated in Fig. 10 also permit assignment of one of the minor olefinic structures observed in this sample. ^1H resonances at 4.66 and 4.85 ppm both give $^1J_{\text{C-H}}$ correlations with a ^{13}C resonance at 113.5 ppm (Fig. 10a). Based on chemical shift alone, this structure is clearly a terminal methylene structure. $^2J_{\text{C-H}}$ and $^3J_{\text{C-H}}$ couplings are observed between this ^{13}C resonance (113.5 ppm) and protons resonating at 1.73 ppm (Fig. 10b). These protons also couple $^2J_{\text{C-H}}-^3J_{\text{C-H}}$ with the quaternary olefinic carbon resonance at 147.7 ppm indicating that this carbon is attached to the protonated olefinic carbon (113.5 ppm). HMQC data (Fig. 10c) indicate that these protons ($^1\text{H}=1.73$ ppm) are directly ($^1J_{\text{C-H}}$) coupled to the ^{13}C resonance at 23.2 ppm. From chemical shift considerations and DEPT data, it is clear that this ^{13}C resonance is due to a methyl group. Hence, overall, these data indicate that the nature of this minor olefin is, as illustrated in Fig. 12, isomeric with the secondary olefin structure described above and illustrated in Fig. 11.

In the case of the fossil Dammar polymer, conventional (Fig. 2 and 3) and two dimensional NMR spectra (Fig. 13) indicate that the most abundant olefin observed is identical to the primary olefin observed in the modern sample (see Fig. 8).

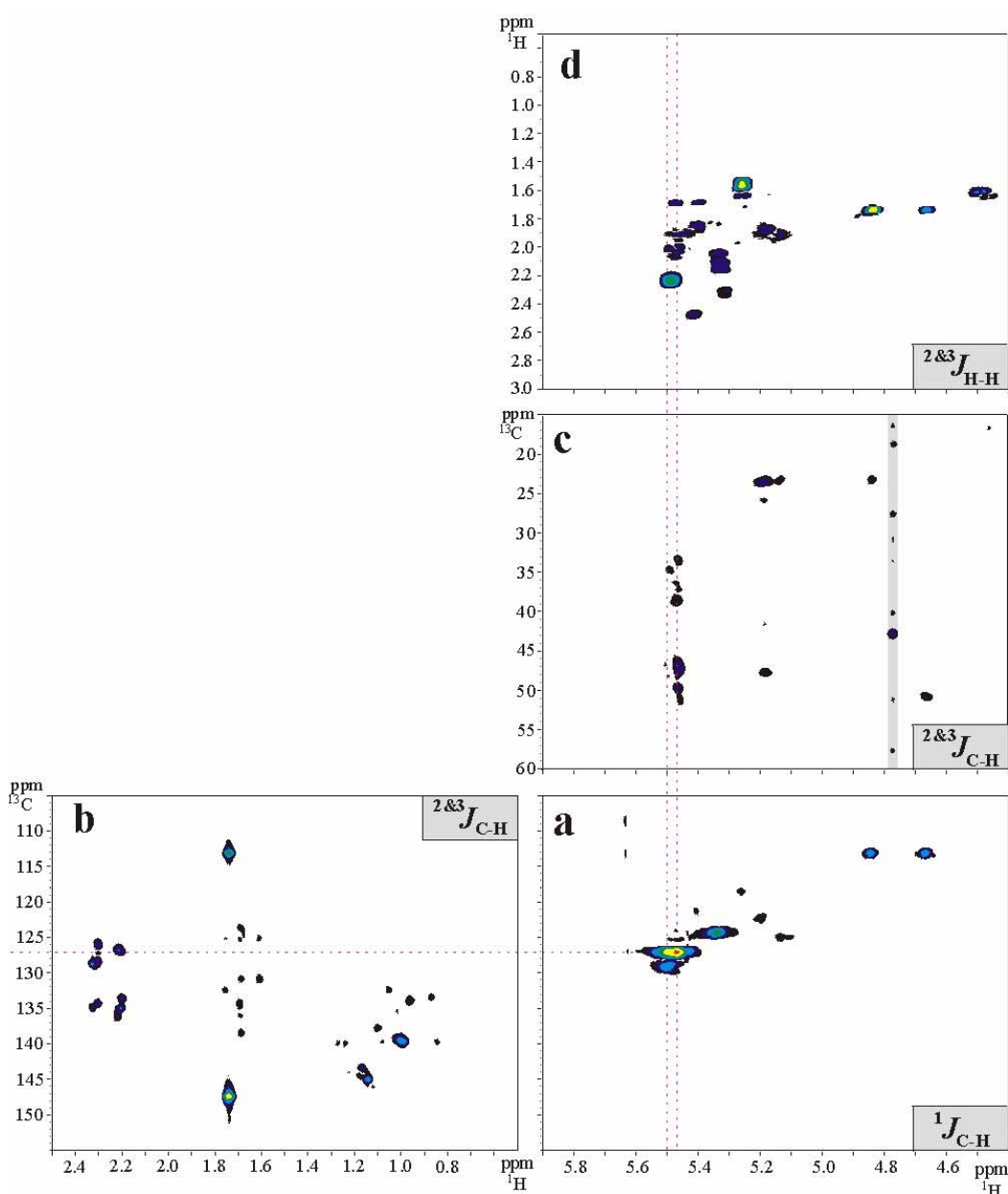


Fig. 13 2D ^{13}C - ^1H NMR spectra for fossil Dammar polymer. (a) HMQC, (b) and (c) HMBC and (d) COSY. Resonances due to the primary olefinic structure are indicated by dashed lines. Click on the image or [here](#) to access a larger view.

The secondary olefin observed in the modern sample, however, is much less abundant in the fossil polymer. It is not possible from the present data to determine if this difference is sample or maturity related. The ^1H spectrum of this sample shows an apparent strong resonance centered at ~ 5.33 ppm which is not significant in the corresponding data for the modern sample. HMQC data for the fossil polymer suggest that this proton is coupled to the ^{13}C resonating at 124.3 ppm. However, one dimensional ^{13}C data for this sample indicate no strong single resonance at this chemical shift. Rather, these data indicate at least 4 partially resolved ^{13}C resonances between 125 and 124 ppm. Furthermore, higher resolution HMQC measurements of this correlation show that the ^1H resonance observed in the 1D ^1H data for this sample is in fact composed of at least 4 unresolved resonances.

As a result of the coincidence of these resonances it is not possible to develop detailed connectivity arguments for these signals. Clearly these signals derive from a family of closely related structural elements (at least in terms of ^1H and ^{13}C chemical shifts). However, it is possible to derive limited information about the structural characteristics of the olefins contributing to these overlapping resonances from COSY data. In this case, $^3J_{\text{H-H}}$ correlations with the multiple resonance at ~ 5.33 ppm are observed at 5.47 ppm (suggesting the presence of a 1,2-diprotonated olefin), and 2.11 and 2.15 ppm (doublet) suggesting that at least one of these olefinic protons is located α to a protonated (probably methine) carbon. Further analysis of these olefins is limited by the overlap of their respective ^{13}C and ^1H resonances, but their diversity itself suggests that a variety of possible pathways are being followed during maturation of these polymers.

One and two dimensional spectra from both the modern and fossil polymers indicate the presence of a number of other minor olefins. In addition to evidence for 1,2-disubstituted (diprotonated) olefins, (discussed above) resonances attributable to minor amounts of terminal and/or *exo*-olefins are also observed. However, due to the weakness of the resonances attributable to these structures, no further analysis of these structures has been attempted at this time.

Conclusions

The nature of the olefinic structures present in the high MW fraction of both modern and fossil Dammar resins is inconsistent with the current widely held "polycadinene" model for these materials. Nor can the data be accommodated within any simple double bond isomer of the existing "polycadinene" model. Additional investigations are necessary to define the precise structural characteristics of these polymers, but it is clear that the existing model is inadequate and requires revision. Data generated in these analyses also suggest that although individually minor, in sum, functionalized structures (especially O-containing ones) may contribute significantly to the overall characteristics and reactivity of these polymers and should not be wholly neglected when describing these materials.

Acknowledgements

The authors wish to express their appreciation to Mr William Lambert for technical assistance in preparation of the polymers, and to Dr David J. Clifford for helpful comments during preparation of this manuscript. Mr Nabil Mailloux of Advanced Chemistry Development Inc. (www.acdlabs.com) is thanked for his assistance in the preparation of JCAMP-DX format NMR data files. The support of the U.S. Dept. of Energy, Office of Basic Energy Sciences, under contract No W-31-109-ENG-38 is also gratefully acknowledged.

References

- 1 D. J. Clifford, P. G. Hatcher, J. V. Muntean, R. E. Botto and K. B. Anderson, The Nature and Fate of Natural Resins In the Geosphere. IX. Structure and maturation similarities of soluble and insoluble polyabdanoids isolated from Tertiary Class I resinites, *Org. Geochem.*, 1999, **30**(7), 635.
- 2 B. G. K. van Aarssen, Q. Zhang and J. W. de Leeuw, An unusual distribution of bicadinanes, tricadinanes, and oligocadinanes in sediments from the Yacheng gasfield, China, *Org. Geochem.*, 1992a, **18**, 805.
- 3 B. G. K. van Aarssen, J. K. C. Hessels and J. W. de Leeuw, The occurrence of polycyclic sesqui-, tri-, and oligoterpenoids derived from a resinous polymeric cadinene in crude oils from southeast Asia, *Geochim. Cosmochim. Acta*, 1992b, **56**(3), 1231.
- 4 J. A. Curiale, P. Kyi, I. D. Collina, A. Din, K. Nyein, M. Nyunt and C. J. Stuart, The Central Myanmar (Burma) oil family-composition and implications for source, *Org. Geochem.*, 1994, **22**(2), 237.
- 5 A. P. Murray, R. E. Summons, C. J. Boreham and L. M. Dowling, Biomarker and n-alkane isotope profiles for tertiary oils: relationship to source rock depositional setting, *Org. Geochem.*, 1994, **22**(3-5), 521.
- 6 C. Armanios, R. Alexander, I. B. Sosrowidjojo and R. I. Kagi, Identification of bicadinanes in Jurassic organic matter from the Eromanga Basin, Australia, *Org. Geochem.*, 1995, **23**(9), 837.
- 7 S. D. Killops, J. I. Raine, A. D. Woolhouse and R. J. Weston, Chemostratigraphic evidence of higher-plant evolution in the Taranaki Basin, New Zealand, *Org. Geochem.*, 1995, **23**(5), 249.
- 8 S. A. Stout, Resin-derived hydrocarbons in fresh and fossil Dammar resins and Miocene rocks and oils in the Mahakam Delta, Indonesia, *ACS Symp. Ser.*, 1995, **617**(Amber, Resinite, and Fossil Resins), 43.
- 9 R. E. Summons, C. J. Boreham, C. B. Foster, A. P. Murray and J. D. Gorter, Chemostratigraphy and the composition of oils in the Perth Basin, western Australia, *APEA J.*, 1995, **35**, pt. 1, 613.
- 10 I. B. Sosrowidjojo, A. P. Murray, R. Alexander, R. I. Kagi and R. E. Summons, Bicadinanes and related compounds as maturity indicators for oils and sediments, *Org. Geochem.*, 1996, **24**(1), 43.
- 11 W. Brackman, K. Spaargaren, J. P. C. M. Van Dongen, P. A. Couperus and F. Bakker, Origin and structure of the fossil resin from an Indonesian Miocene coal, *Geochim. Cosmochim. Acta*, 1984, **48**(12), 2483.
- 12 B. G. K. van Aarssen, H. C. Cox, P. Hoogendoorn and J. W. de Leeuw, A cadinene biopolymer in fossil and extant Dammar resins as a source for cadinanes and bicadinanes in crude oils from South-East Asia, *Geochim. Cosmochim. Acta*, 1990, **54**(11), 3021.
- 13 B. G. K. van Aarssen, J. W. de Leeuw and B. Horsfield, A comparative study of three different pyrolysis methods used to characterize a biopolymer isolated from fossil and extant Dammar resins, *J. Anal. Appl. Pyrolysis*, 1991, **20**, 125.
- 14 B. G. K. van Aarssen and J. W. de Leeuw, High-molecular-mass substances in resinites as possible precursors of specific hydrocarbons in fossil fuels, *Org. Geochem.*, 1992, **19**(4-6), 315.
- 15 B. G. K. van Aarssen, J. W. de Leeuw, M. Collinson, J. J. Boon and K. Goth, Occurrence of polycadinene in fossil and recent resins, *Geochim. Cosmochim. Acta*, 1994, **58**(1), 223.
- 16 J. S. Mills and A. E. A. Werner, The chemistry of Dammar resin, *J. Chem. Soc.*, 1955, 3132.
- 17 J. S. Mills, The constitution of the neutral, tetracyclic triterpenes of Dammar resin, *J. Chem. Soc.*, 1956, 2196.

- 18 E. Rene de la Rie, Stable varnishes for old master paintings, PhD Thesis, University of Amsterdam, 1988.
- 19 K. B. Anderson and R. E. Winans, The nature and fate of natural resins in the geosphere. I. Evaluation of pyrolysis-gas chromatography-mass spectrometry for the analysis of natural resins and resinates, *Anal. Chem.*, 1991, **63**, 2901.
- 20 D. M. Doddrell, D. T. Pegg and M. R. Bendall, Distortionless enhancement of NMR signals by polarization transfer, *J. Magn. Reson.*, 1982, **48**, 323.
- 21 A. J. Shaka, J. Keeler and R. Freeman, Evaluation of a new broadband decoupling sequence: WALTZ-16, *J. Magn. Reson.*, 1983, **53**(2), 313.
- 22 A. J. Shaka, J. Keeler, T. Frenkiel and R. Freeman, An improved sequence for broadband decoupling: WALTZ-16, *J. Magn. Reson.*, 1983, **52**(2), 335.
- 23 Z. Starcuk and V. Sklenar, Composite pulse sequences with variable performance, *J. Magn. Reson.*, 1985, **62**(1), 113.
- 24 W. P. Aue, E. Bartholdi and R. R. Ernst, Two-dimensional spectroscopy. Application to nuclear magnetic resonance, *J. Chem. Phys.*, 1976, **64**(5), 2229.
- 25 K. Nagayama, A. Kumar, K. Wuethrich and R. R. Ernst, Experimental techniques of two-dimensional correlated spectroscopy, *J. Magn. Reson.*, 1980, **40**(2), 321.
- 26 A. Bax, R. H. Griffey and B. L. Hawkins, Correlation of proton and nitrogen-15 chemical shifts by multiple quantum NMR, *J. Magn. Reson.*, 1983, **55**(2), 301.
- 27 A. Bax and S. Subramanian, Sensitivity-enhanced two-dimensional heteronuclear shift correlation NMR spectroscopy, *J. Magn. Reson.*, 1986, **67**(3), 565.
- 28 A. Bax and M. F. Summers, Proton and carbon-13 assignments from sensitivity-enhanced detection of heteronuclear multiple-bond connectivity by 2D multiple quantum NMR, *J. Am. Chem. Soc.*, 1986, **108**(8), 2093.
- 29 A. J. Shaka, P. B. Barker and R. Freeman, Computer-optimised decoupling scheme for wideband applications and low-level operation, *J. Magn. Reson.*, 1985, **64**(3), 547.
- 30 Atta-ur-Rahman and V. U. Ahmad, *¹³C-NMR of natural products. Volume 1. Monoterpenes and Sesquiterpenes*, Plenum Press, New York, 1991.

Paper b000495m